Regular Article

PHYSICAL CHEMISTRY RESEARCH
Published by the
Iranian Chemical Society
www.physchemres.org
info@physchemres.org

Phys. Chem. Res., Vol. 10, No. 4, 571-579, December 2022
DOI: 10.22036/PCR.2022.327519.2024

Calculation of Structural Parameters and Diffusion Coefficient of Sodium Dodecyl Sulfate at Concentrations Lower and Higher Than the Critical Micelle Concentration in the Presence of Amyloid-Beta Peptide

A. Saghiri, M.R. Bozorgmehr* and A. Morsali

Department of Chemistry, Mashhad Branch, Islamic Azad University, Mashhad, Iran

(Received 1 February 2022, Accepted 23 March 2022)

Sodium dodecyl sulfate (SDS) solution is considered a cell membrane mimicking solution. In this study, the effect of the amyloid-beta peptide on the structure and diffusion coefficient of SDS was investigated by molecular dynamics simulation. To control the accuracy of the calculations, a micelle containing 60 molecules of SDS was simulated. The radius of gyration and the moment of inertia of the micelle were calculated and compared with the experimental and simulation results. The results obtained were in good agreement with the experimental and simulation results. The simulations in the presence of amyloid-beta were performed at two concentrations of SDS, below and above the critical micelle concentration. The results showed that as the concentration of SDS increased, the diffusion coefficient of peptide and sodium ion increased while the diffusion coefficient of water and SDS decreased. The calculation of the moments of inertia in different directions showed that the micelles deviated from the ellipsoidal shape at sub-critical micelle concentrations of SDS.

Keywords: Membrane, Mobility, Alzheimer, Radius of gyration, Transport properties

INTRODUCTION

Alzheimer's is one of the most progressive brain disorders. It is claimed that this disease will cost about $ 1.08 trillion by 2050, only in the United States [1]. Pathologically, two reasons have been identified for the disease: formation of neurofibrillary tangles from filaments of microtubule-associated highly phosphorylated tau proteins and aggregation of amyloid plaques [2]. Today, the pathological approach to Alzheimer's disease is reformulated and focuses on the role of soluble aggregates as the molecular form of the amyloid-beta peptide [3]. Amyloid-beta peptide is a fragment with 39 to 43 residues produced from proteolytic fragmentation of membrane-associated amyloid precursor protein [4]. Of the fragments with 39 to 43 residues, the amyloid-beta peptide with 42 residues, *i.e.* Aβ (1 - 42), accumulates more rapidly than the other ones [5]. While the N-terminal of the Aβ (1 - 42) peptide has a hydrophilic nature, its C-terminal has a hydrophobic nature. When Aβ (1 - 42) is isolated from the amyloid precursor protein, the C-terminal of the peptide is in the membrane [6]. As the Aβ (1 -42) peptide moves away from the membrane, its conformation changes. Changing the conformation of the Aβ (1 - 42) peptide increases its rate of accumulation. It has been shown that the membrane is involved in the process of peptide accumulation [7,8]. Many experimental and computational efforts have been made to investigate the membrane interaction with the amyloid peptide [9,10]. It has been found that the interaction between the membrane and the amyloid peptide changes the rate of diffusion of different species [11]. Also, Aβ (1 - 42) diffusion in the presence of membrane components was found to increase neurotoxic effects [12]. However, the mechanism of the interaction between amyloid peptide and the membrane remains unclear [13].

Sodium dodecyl sulfate (SDS) micelles are used as membrane-mimicking environments [14]. In many cases, SDS has been used as a membrane-like environment for the

*Corresponding author. E-mail: bozorgmehr@mshdiau.ac.ir

accumulation of the amyloid peptide. It was shown that the soluble oligomers stabilized and fibril growth enhanced at neutral pH and near the critical micelle concentration (CMC) of SDS [15]. Also, amyloid peptide accumulation increased in the presence of 2 mM SDS [16]. Nuclear magnetic resonance (NMR) spectroscopy showed that diffusion coefficients of SDS and amyloid peptide did not significantly change with changes in the size of SDS micelle [17]. Despite all these efforts, various experimental methods have failed to provide a complete description of the structure and assembly of the amyloid peptide for various reasons, including the disorder properties of amyloid peptide, high accumulation propensity, and the immense heterogeneous accumulation [1]. In addition, common experimental methods in the study of amyloid peptides, such as NMR, transmission electron microscopy (TEM), atomic force microscopy (AFM), and circular dichroism (CD), generally provide space- and time-averaged properties. Thus, molecular dynamics simulation by tracking different length and time scales can complement experimental methods.

In this study, the self-aggregation of SDS molecules around the amyloid peptide was investigated using all-atom molecular dynamics simulations. Sub- and super-critical concentrations of SDS were used. Calculations were performed with one monomer of the amyloid peptide at different concentrations of SDS and six monomers of amyloid peptides at the same concentrations. For comparison, molecular dynamics simulation was repeated in the absence of amyloid peptide. For the analysis of the calculations, the diffusion coefficients of different species in the designed systems were calculated.

METHOD

GROMOS 43A1 force field [18] and GROMACS 5.1.2 [19] were used for calculations. The molecular dynamics simulation was performed in two parts. First, part calculations were performed to control the accuracy of the simulations. In this step of the calculation, the protocol presented in [20] was used. Also, the checklist presented in [21] was used to calculate the diffusion coefficients. In the first part, a micelle containing 60 molecules of SDS was simulated. The aggregation number of 60 [22] was close to the experimental value of 63 at the CMC and in accordance with the number used in other SDS simulations [23,24]. Micelle Maker [25] was used to build the initial micellar structure. The designed micelle structure is shown in Fig. 1.

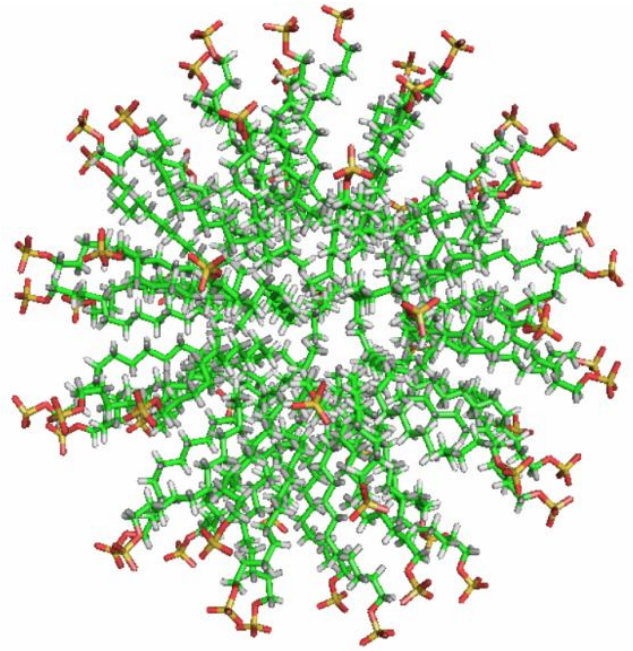

Fig. 1. The designed micelle structure containing 60 molecules of SDS.

The micelles were placed in a cubic box. The distance of the edges of the box from the micelle surface was assumed to be 1 nm. The designed simulation box was filled with simple point charge (SPC) water molecules [26]. Sodium counterions were added to the box to neutralize the total charge of the system. Berendsen weak coupling thermostat [27] was used to control temperature (300 K) and pressure (1 bar). A cutoff scheme (1.4 nm) was used for van der Waals interactions, and the electrostatic interaction was computed using the particle-mesh Ewald method [28]. LINCS [29] and SETTLE [30] algorithms were used to constrain surfactant bond lengths and water geometry, respectively. In order to keep the maximum force on any atom below 2000 kJ mol^{-1}, energy minimization was performed before and after the addition of sodium ions and SPC water molecules. Also, the relaxation of water molecules around the micelle position was achieved by harmonically restraining SDS head group atoms with a

force constant of 1000 kJ mol^{-1}. In the final step, molecular dynamics simulation was performed for 10 ns with a 2-fs time step. Because the force field parameters of SDS are not provided by default in the GROMACS package, these parameters were calculated using the PRODRG server [31]. To create an input on this web server, the optimized structure of SDS is needed. The structure of the SDS molecule was optimized using the B3LYP density-functional theory method and 6-31G basis set. To ensure the optimization of structures, frequency calculations were performed using the same method and the same previous function. The results showed that there were no virtual frequencies for the optimal structures. The calculations in this step were done using the GAMESS software [32]. The optimized structures of SDS molecules are shown in In the second phase, four simulation boxes were designed. One peptide was placed in the first and second boxes, and six peptides were placed in the third and fourth boxes. The initial structure of Aβ (1 - 42) was taken from the protein data bank with accession code 1Z0Q [33]. In the first and second boxes, 40 and in the third and fourth boxes, 80 SDS molecules were placed randomly. Values of 40 and 80 SDS molecules were considered for concentrations lower and higher than CMC, respectively. Boxes were filled with SPC water molecules. Then, each simulation box was neutralized with sodium ions. The systems designed at this stage were named $S_{i,j}$, in which i and j represent the number of peptides and SDSs in the simulation box, respectively.

Thus, i took values of 1 and 6, and j took values of 40 and 80. For example, system S_1, 80 represented a simulation box containing 1 peptide and 80 SDSs. At this step, simulations were performed by considering the first step protocol. However, the simulation time was 200 nanoseconds. To avoid any dependency on the initial conditions and increase the accuracy of the simulations, each simulation was repeated four times under different initial conditions.

RESULTS AND DISCUSSION

In Fig. 2, the optimized structure of SDS is shown. Since SDS force field parameters are not present by default in the GROMACS package, a PRODRG server was used to determine these parameters. The partial charges used on the PRODRG server are estimated charges; thus, they can have a great effect on the simulation results. For this purpose, the partial charges of the atoms forming the SDS were calculated by the Charges from Electrostatic Potentials using a Grid-based method (GHELPG) [34]. The partial charges obtained for the SDS atoms are shown in Fig. 2. In addition to the partial charges of atoms, the torsional topology parameters of SDS were manually adjusted. Also, the Ryckaert-Bellemans potential function was used to optimize the dihedral parameters of the alkyl tail of SDS. To investigate the validity of the simulations performed, the radius of gyration (Rg) and the moments of inertia of the micelle were calculated in a final nanosecond of the first part of the simulation. The results are shown in Figs. 3 and 4, respectively.

As Figs. 3 and 4 show, there was a good agreement between the obtained results, the simulations data [20, 23, 24,35], and experimental values [36]. Furthermore, a $I_1 \approx I_2 < I_3$ relationship was observed between moments of inertia in different principal axes. This indicates that the micellar shape was an oblate ellipsoid, which was in line with the experimental evidence. For the sampling of the simulated systems in Part II, free-energy landscape (FEL) analysis was used [37]. The following were done as the three main steps of FEL analysis: a) Two principal components, such as root-mean-square-deviation (RMSD)

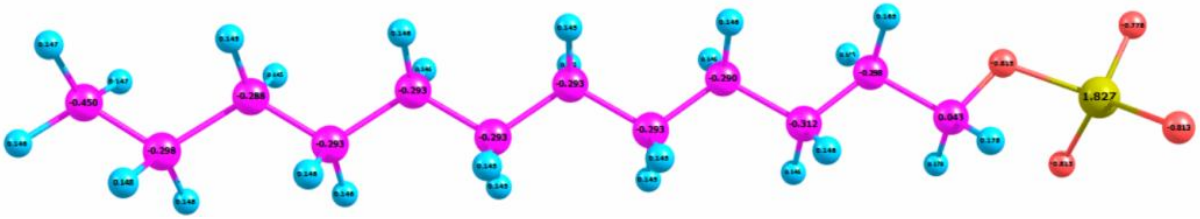

Fig. 2. The optimized structures of SDS molecules along with the partial charges of atoms.

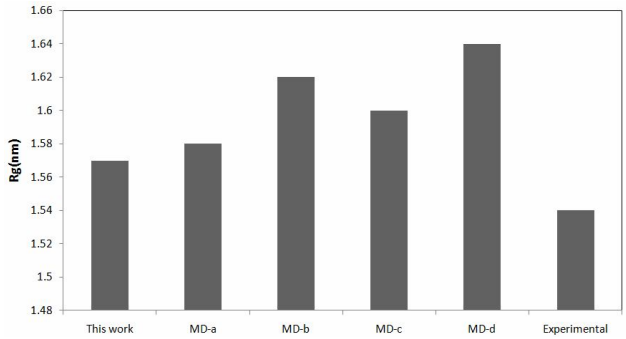

Fig. 3. The radius of gyration (Rg) of the micelle containing 60 molecules of SDS in the absence of amyloid-beta peptide, MD-a [20], MD-b [24], MD-c [23], and MD-d [35].

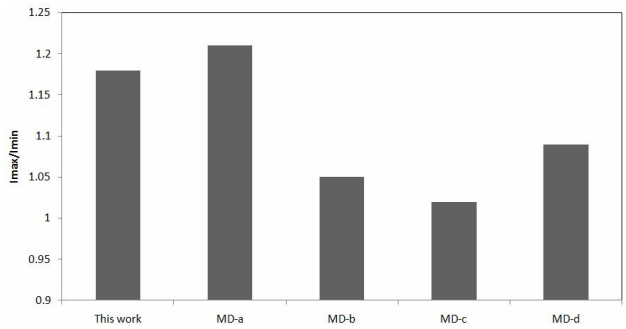

Fig. 4. The I_{max}/I_{min} of micelle containing 60 molecules of SDS in the absence of amyloid-beta peptide, MD-a [20], MD-b [24], MD-c [23], and MD-d [35].

and the radius of gyration (Rg) were calculated; b) the possibility of the presence of system configuration in every corresponding value of principal component 1 (PC1) and component 2 (PC2) was obtained; c) the free-energy configurations were calculated based on the probability values. The result of the FEL analysis for the system S_1, 40 is shown in Fig. 5.

In Fig. 5, the red and blue zones correspond to the highest and lowest free energy values, respectively. Similar figures were obtained for other systems, but they are not shown here due to the space limitation. Samples were selected from the minimum free energy values. In Fig. 6, the structures of systems S_1, 40 and S_1, 80 are shown.

According to Fig. 6, increasing the amount of SDS destabilized the secondary structure of the peptide; as a

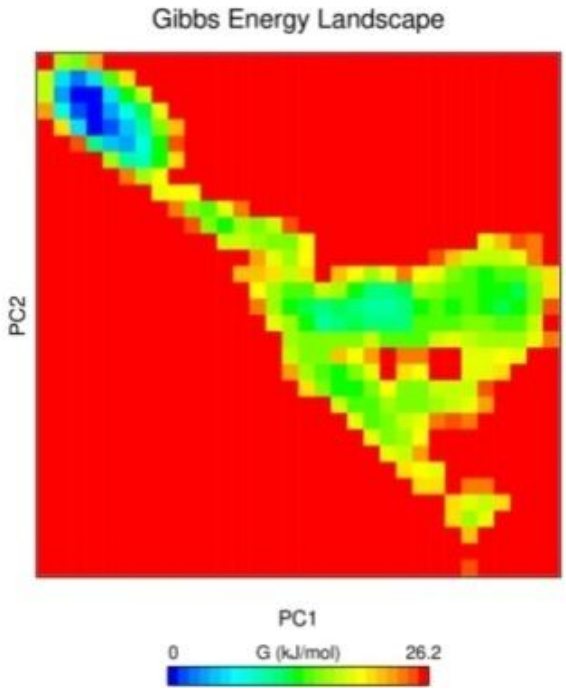

Fig. 5. The result of the FEL analysis for system S_1, 40.

result, the long alpha-helical region in the system S_1, 40 was transformed into two short alpha-helices in the system S_1, 80. In fact, the middle part of the helix became a random coil. Another point to note is that while the peptide was U-shaped in the system S_1, 40, it was S-shaped in the system S_1, 80, it is. According to Fig. 6, it seems that the aggregate structures formed around the peptide in both systems were approximately similar, but the shapes of the micelles were different in three dimensions. To illustrate this, the ratios of moments of inertia in different directions for the micelles were calculated. The results are listed in Table 1. The ratios reported in Table 1 are averaged over the last 5 ns. The ratios of moments of inertia for the system S_1, 40, indicate that the shape of the aggregate structure was nearly ellipsoidal whereas the ratios of moments of inertia for the system S_1, 80, show that the shape of the aggregate structure deviated greatly from the ellipsoidal shape. In Fig. 6, this difference is less pronounced in the aggregate structures because the viewing angle in the shape is adjusted so that the peptide structure and the changes in it are visible. Fig. 7 illustrates the structures of systems S_6, 40 and S_6, 80 is shown.

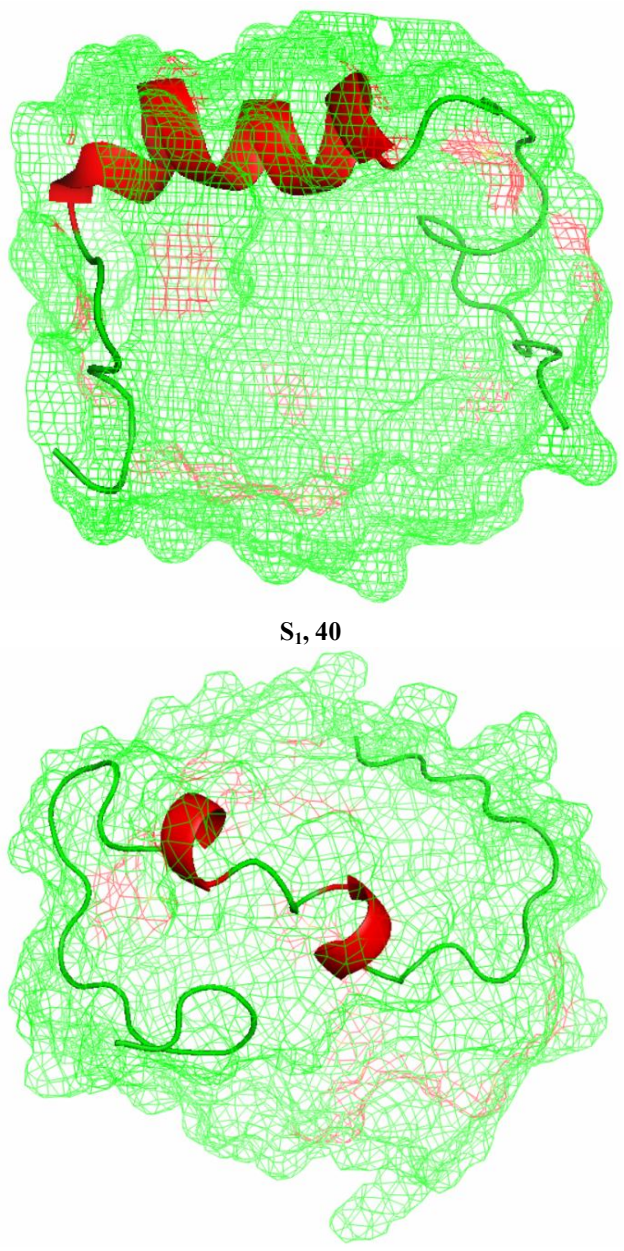

Fig. 6. The structure of SDS micelle along with amyloid-beta peptide in systems S_1, 40 and S_1, 80.

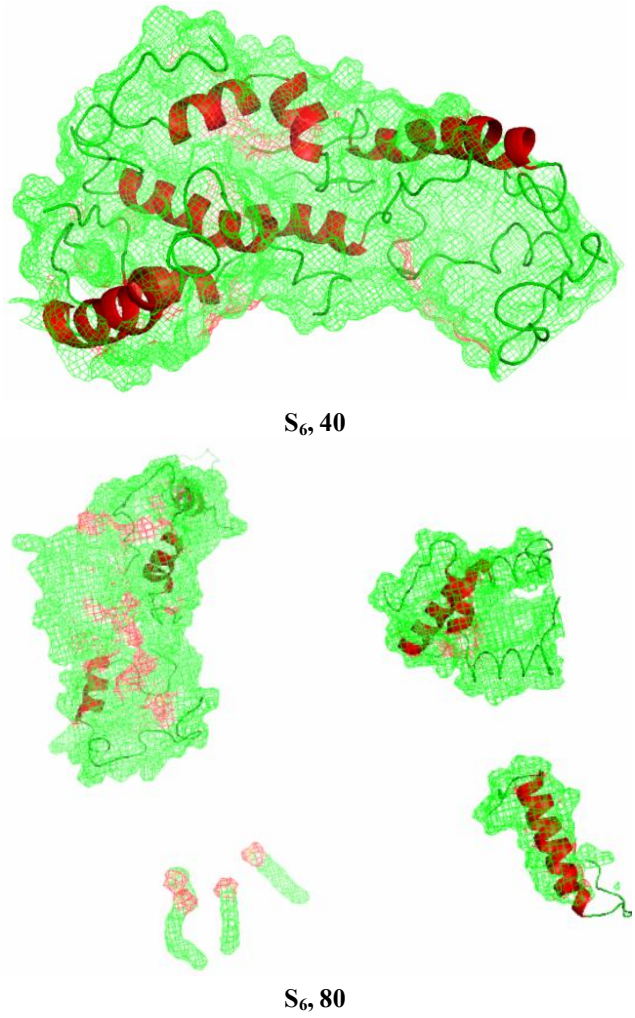

Fig. 7. The structure of SDS micelle along with amyloid-beta peptides in systems S_6, 40 and S_6, 80.

According to Fig. 7, no peptide aggregation was observed when the concentration of SDS was increased to a level higher than the CMC. At a higher concentration than the CMC, the peptides were divided into three sets, evidenced by a ternary, a binary, and a monomeric structure. Moreover, it was observed that at a higher concentration than the CMC, two peptides lost their secondary structures and the helix structure became coiled. However, at a lower concentration than the CMC, one peptide lost its secondary structure and the helix structure became coiled. The ratios of moments of inertia in different directions for the micelles of systems S_6, 40 and S_6, 80 are listed in Table 1.

For the micelles in the system S_6, 80, the micelle structure with the largest number of peptides was considered for

Table 1. Ratios of Moments of Inertia of SDS Micelles in the Studied Systems

System	I_3/I_1	I_3/I_2	I_2/I_1
S_1, 40	1.40	1.08	1.26
S_1, 80	3.00	1.07	2.79
S_6, 40	3.51	1.08	3.23
S_6, 80	1.91	1.38	1.39

further analysis. It was also observed that while the micelles deviated utterly from an ellipsoidal shape in the system S_6, 40, they were somewhat ellipsoidal in the system S_6, 80. The Einstein relation was used to calculate the diffusion coefficients of components in all simulated systems:

$$D = \frac{1}{6}\lim_{t\to\infty}\frac{d}{dt}\langle|r_i(t) - r_i(0)|^2\rangle \quad (1)$$

where r_i is the atom coordinate vector and the term inside the angle brackets is the mean square displacement (MSD). In this approach, the self-diffusion coefficient (D) is proportional to the slope of the MSD as a function of time in the diffusional regime [38]. The calculated diffusion coefficient values are listed in Table 2.

To obtain error ranges, the diffusion coefficients for 20 separate 20 ps segments were obtained and averaged, and the standard deviation was calculated. The linear range of the MSD plot was used to calculate the diffusion coefficients of different components other than water. The MSD plot of water in all areas was linear. Also, the last five nanoseconds of the simulation were used to determine the MSD plot. According to the values reported in Table 2, the diffusion coefficients of sodium ion and peptide at higher concentrations of SDS were higher than those of sodium ion and peptide at low concentrations of SDS. The diffusion coefficients of water molecules and SDS followed the opposite trend. Since the diffusion coefficient of a single sodium ion in water is $2.2 \pm 0.4 \times 10^{-5}$ cm^2 s^{-1}, the decrease in the diffusion coefficient of sodium ions in the presence of the peptide indicates that the sodium ions interacted with the head group of the SDS. The higher mobility of the peptide in the presence of higher concentrations of SDS suggests that the probability of peptide accumulation decreased when it interacted with the membrane.

CONCLUSIONS

As amyloid-beta moves away from the surface of the cell membrane, its conformation changes and becomes susceptible to structural aggregation. The aggregate structure of amyloid-beta causes Alzheimer's disease by creating amyloid plaques. On the other hand, the solution containing SDS is a membrane mimicking solution. Also, the interaction between SDS and peptides differs at lower and higher concentrations of the CMC. To investigate the effects of the amyloid-beta peptide on SDS, molecular dynamics simulations were performed at concentrations lower and higher than the CMC in the presence of one and six peptides. The results showed that the peptide and sodium dodecyl sulfate has mutual interactions. As such, the peptide affects the diffusion coefficient of sodium dodecyl sulfate and the SDS changes the structure of the peptide. The presence of amyloid-beta peptide reduced the diffusion coefficient of SDS at concentrations higher than the CMC. On the other hand, the shape of the aggregate structure obtained from SDS deviated from an ellipsoidal shape. This change in the structure of SDS also affected the number of peptides. Accordingly, in the presence of six peptides, instead of a large aggregate structure, smaller aggregate

Table 2. Diffusion Coefficient Values ($D \times 10^{-5}$ cm^2 s^{-1}) of Sodium Ion, SDS, Water, and Amyloid-Beta peptide

System	Na^+	SDS	Water	Peptide
S_1, 40	0.18 (± 0.15)	0.12 (± 0.10)	4.17 (± 0.10)	0.06 (± 0.08)
S_1, 80	1.951 (± 0.15)	0.02 (± 0.10)	4.08 (± 0.10)	0.25 (± 0.08)
S_6, 40	1.05 (± 0.15)	0.03 (± 0.10)	3.78 (± 0.10)	0.04 (± 0.08)
S_6, 80	1.30 (± 0.15)	0.01 (± 0.10)	3.70 (± 0.10)	0.162 (± 0.08)

structures were formed. SDS, on the other hand, altered the secondary structure of the amyloid-beta peptide. Thus, at concentrations higher than the CMC, the helix secondary structure of amyloid-beta peptide is shortened. On the other hand, the diffusion coefficient of the peptide decreased with a decrease in the SDS concentration. The results of this research can shed some light on the mechanism of beta-amyloid accumulation. Given that in this study concentrations higher and lower than the CMC were considered, the findings of this study can deepen our understanding of the process of peptide transfer from the membrane surface. In practice, the transfer of the peptide from the surface of the membrane causes its structure to change and aggregate, which, in turn, causes Alzheimer's disease. Given that intermolecular forces, especially hydrophobic forces, play a key role in amyloid-beta aggregation, further studies are required to investigate the effects of these forces on the process of amyloid-beta aggregation.

REFERENCES

[1] Nasica-Labouze, J.; Nguyen, P. H.; Sterpone, F.; Berthoumieu, O.; Buchete, N.- V.; Cote, S.; De Simone, A.; Doig, A. J.; Faller, P.; Garcia, A., Amyloid β protein and Alzheimer's disease: When computer simulations complement experimental studies. *Chem. Rev.* **2015**, *115*, 3518-3563, DOI: 10.1021/cr500638n.

[2] Hardy, J.; Selkoe, D. J., The amyloid hypothesis of Alzheimer's disease: progress and problems on the road to therapeutics. *Sci.* **2002**, *297*, 353-356, DOI: 10.1126/science.1072994.

[3] Broersen, K.; Rousseau, F.; Schymkowitz, J., The culprit behind amyloid beta peptide related neurotoxicity in Alzheimer's disease: oligomer size or conformation? Alzheimer's. *Res. Ther.* **2010**, *2*, 1-14, DOI: 10.1186/alzrt36.

[4] Fändrich, M.; Schmidt, M.; Grigorieff, N., Recent progress in understanding Alzheimer's β-amyloid structures. *Trends Biochem. Sci.* **2011**, *36*, 338-345, DOI: 10.1016/j.tibs.2011.02.002.

[5] Okamoto, A.; Yano, A.; Nomura, K.; Higai, Si.; Kurita, N., Stable conformation of full-length amyloid-β (1 - 42) monomer in water: Replica exchange molecular dynamics and *ab initio* molecular orbital simulations. *Chem. Phys. Lett.* **2013**, *577*, 131-137, DOI: 10.1016/j.cplett.2013.05.057.

[6] Haass, C.; Selkoe, D. J., Soluble protein oligomers in neurodegeneration: lessons from the Alzheimer's amyloid β-peptide. *Nat. Rev. Mol. Cell Biol.***2007**, *8*, 101-112, DOI: 10.1038/nrm2101.

[7] Bokvist, M.; Lindström, F.; Watts, A.; Gröbner, G., Two types of Alzheimer's β-amyloid (1 - 40) peptide membrane interactions: aggregation preventing transmembrane anchoring versus accelerated surface fibril formation. *J. Mol. Biol.* **2004**, *335*, 1039-1049, DOI: 10.1016/j.jmb.2003.11.046.

[8] Dante, S.; Hauss, T.; Dencher, N. A., Insertion of externally administered amyloid β peptide 25-35 and perturbation of lipid bilayers. *Biochem.***2003**, *42*, 13667-13672, DOI: 10.1021/bi035056v.

[9] Smeralda, W.; Since, M.; Cardin, J.; Corvaisier, S.; Lecomte, S.; Cullin, C.; Malzert-Fréon, A., β-Amyloid peptide interactions with biomimetic membranes: A multiparametric characterization. *Int. J. Biol. Macromol.* **2021**, *181*, 769-777, DOI: 10.1016/j.ijbiomac.2021.03.107.

[10] Williams, T. L.; Serpell, L.C., Membrane and surface interactions of Alzheimer's Aβ peptide-insights into the mechanism of cytotoxicity. *The FEBS J.* **2011**, *278*, 3905-3917, DOI: 10.1111/j.1742-4658.2011.08228.x.

[11] Kayed, R.; Sokolov, Y.; Edmonds, B.; McIntire, T. M.; Milton, S. C.; Hall, J. E.; Glabe, C. G., Permeabilization of lipid bilayers is a common conformation-dependent activity of soluble amyloid oligomers in protein misfolding diseases. *J. Biol. Chem.* **2004**, *279*, 46363-46366, DOI: 10.1074/jbc.C400260200.

[12] Kirkitadze, M. D.; Bitan, G.; Teplow, D. B., Paradigm shifts in Alzheimer's disease and other neurodegenerative disorders: the emerging role of oligomeric assemblies. *J. Neurosci. Res.* **2002**, *69*, 567-577, DOI: 10.1002/jnr.10328.

[13] Sureshbabu, N.; Kirubagaran, R.; Jayakumar, R., Surfactant-induced conformational transition of amyloid β-peptide. *Eur. Biophys. J.* **2009**, *38,* 355,

DOI: 10.1073/pnas.90.22.10573.

[14] Wahlström, A.; Hugonin, L.; Perálvarez-Marín, A.; Jarvet, J.; Gräslund, A., Secondary structure conversions of Alzheimer's Aβ (1 - 40) peptide induced by membrane-mimicking detergents. *The FEBS J.***2008**, *275*, 5117-5128, DOI: 10.1111/j.1742-4658.2008.06643.x.

[15] Yamamoto, S.; Hasegawa, K.; Yamaguchi, I.; Tsutsumi, S.; Kardos, J.; Goto, Y.; Gejyo, F.; Naiki, H., Low concentrations of sodium dodecyl sulfate induce the extension of β2-microglobulin-related amyloid fibrils at a neutral pH. *Biochem.* **2004**, *43*, 11075-11082, DOI: 10.1021/bi049262u.

[16] Rangachari, V.; Reed, D. K.; Moore, B. D.; Rosenberry, T. L., Secondary structure and interfacial aggregation of amyloid-β (1- 40) on sodium dodecyl sulfate micelles. *Biochem.***2006**, *45*, 8639-8648, DOI: 10.1021/bi060323t.

[17] Jarvet, J.; Danielsson, J.; Damberg, P.; Oleszczuk, M.; Gräslund, A., Positioning of the Alzheimer Aβ (1 - 40) peptide in SDS micelles using NMR and paramagnetic probes. *J. Biomol. NMR* **2007**, *39*, 63-72, DOI: 10.1007/s10858-007-9176-4.

[18] Lier, B.; Öhlknecht, C.; Ruiter, A. D.; Gebhardt, J.; Gunsteren, W. F.; Oostenbrink, C.; Hansen, N., A suite of advanced tutorials for the GROMOS biomolecular simulation software [Article v1. 0]. *Live. Co. M. S.***2020**, *2*, 18552-18552, DOI: 10.33011/ livecoms.2.1.18552.

[19] Abraham, M.; Van Der Spoel, D.; Lindahl, E.; Hess, B., the GROMACS development team. GROMACS user manual version 5: **2014**, 1-298.

[20] Shang, B. Z.; Wang, Z.; Larson, R. G., Molecular dynamics simulation of interactions between a sodium dodecyl sulfate micelle and a poly (ethylene oxide) polymer. *J. Phys. Chem. B* **2008**, *112*, 2888-2900, DOI: 10.1021/jp0773841.

[21] Maginn, E. J.; Messerly, R. A.; Carlson, D. J.; Roe, D. R.; Elliot, J. R., Best practices for computing transport properties 1. Self-diffusivity and viscosity from equilibrium molecular dynamics [article v1. 0]. *Live. Co. M. S.***2019**, *1*, 6324-6324, DOI: 10.33011/livecoms.1.1.6324.

[22] Ahmadzade, A.; Bozorgmehr, M. R.; Parvaee, E., The effect of sodium dodecyl sulfate concentration on the aggregation behavior of Aβ (1 - 42) peptide: Molecular dynamics simulation approach. *J. Mol. Liq.* **2020**, *303*, 112651, DOI: 10.1016/j.molliq.2020.112651.

[23] Del Alba Pacheco-Blas, M.; Vicente, L., Molecular dynamics simulation of removal of heavy metals with sodium dodecyl sulfate micelle in water. *Colloids Surf. A Physicochem. Eng.* **2019**, *578*, 123613, DOI: 10.1016/j.colsurfa.2019.123613.

[24] Bruce, C. D.; Berkowitz, M. L.; Perera, L.; Forbes, M. D., Molecular dynamics simulation of sodium dodecyl sulfate micelle in water: micellar structural characteristics and counterion distribution. *J. Phys. Chem. B* **2002**, *106*, 3788-3793, DOI: 10.1021/jp013616z.

[25] Krüger, D. M.; Kamerlin, S. C., Micelle Maker: An online tool for generating equilibrated micelles as direct input for molecular dynamics simulations. *ACS Omega* **2017**, *2*, 4524-4530, DOI: 10.1021/acsomega.7b00820.

[26] Biswal, J.; Jayaprakash, P.; Rangaswamy, R.; Jeyakanthan, J., Synergistic effects of hydration sites in protein stability: a theoretical water thermodynamics approach. Frontiers in Protein Structure, Function, and Dynamics, Springer, **2020**, pp. 187-212.

[27] Li, T. E.; Nitzan, A.; Subotnik, J. E., Collective vibrational strong coupling effects on molecular vibrational relaxation and energy transfer: Numerical insights *via* cavity molecular dynamics simulations. *Angew. Chem.* **2021**, *133*, 15661-15668, DOI: 10.1002/ange.202103920.

[28] Harvey, M.; De Fabritiis, G., An implementation of the smooth particle mesh Ewald method on GPU hardware. *J. Chem. Theory Comput.* **2009**, *5*, 2371-2377, DOI: 10.1021/ct900275y.

[29] Hess, B., P-LINCS: A parallel linear constraint solver for molecular simulation. *J. Chem. Theory Comput.* **2008**, *4*, 116-122, DOI: 10.1021/ct700200b.

[30] Celebi, A. T.; Barisik, M.; Beskok, A.,Surface charge-dependent transport of water in graphene nano-channels. *Microfluid. Nanofluidics* **2018**, *22*, 1-10, DOI: 10.1007/s10404-017-2027-z.

[31] Schüttelkopf, A. W.; Van Aalten, D. M., PRODRG: a tool for high-throughput crystallography of protein-ligand complexes. *Acta Crystallogr. Sect. D: Biol. Crystallogr.* **2004**, *60*, 1355-1363, DOI: 10.1107/S0907444904011679.

[32] Gordon, M. S.; Schmidt, M. W., Advances in electronic structure theory: GAMESS a decade later. In: Theory and applications of computational chemistry. Elsevier, **2005**, pp. 1167-1189.

[33] Tomaselli, S.; Esposito, V.; Vangone, P.; van Nuland, N. A.; Bonvin, A. M.; Guerrini, R.; Tancredi, T.; Temussi, P. A.; Picone, D., The α-to-β conformational transition of Alzheimer's Aβ-(1 - 42) peptide in aqueous media is reversible: a step by step conformational analysis suggests the location of β conformation seeding. *Chem. Bio. Chem.* **2006**, *7*, 257-267, DOI: 10.1002/cbic.200500223.

[34] Hu, H.; Lu, Z.; Yang, W., Fitting molecular electrostatic potentials from quantum mechanical calculations. *J. Chem. Theory Comput.* **2007**, *3*, 1004-1013, DOI: 10.1021/ct600295n.

[35] Rakitin, A. R.; Pack, G. R., Molecular dynamics simulations of ionic interactions with dodecyl sulfate micelles. *J. Phys. Chem. B* **2004**, *108*, 2712-2716, DOI: 10.1021/jp030914i.

[36] Santos, S. F.; Zanette, D.; Fischer, H.; Itri, R., A systematic study of bovine serum albumin (BSA) and sodium dodecyl sulfate (SDS) interactions by surface tension and small angle X-ray scattering. *J. Colloid Interface Sci.* **2003**, 262, 400-408, DOI: 10.1016/S0021-9797(03)00109-7.

[37] Lei, H.; Wu, C.; Liu, H.; Duan, Y., Folding free-energy landscape of villin headpiece subdomain from molecular dynamics simulations. *Proceedings of the National Academy of Sciences* **2007**, *104*, 4925-4930, DOI: 10.1073/pnas.0608432104.

[38] Frenkel, D.; Smit, B., Understanding molecular simulation: from algorithms to applications. Elsevier, **2001**.